

# STUDY OF PHASE FORMATION AND ATOMIC TRANSPORT IN ION IMPLANTED AND IRRADIATED ALLOYS

## ŠTUDIJA NASTAJANJA FAZ IN TRANSPORTA IMPLANTIRANIH IONOV V OBSEVANIH ZLITINAH

Jacek Jagielski<sup>1,2</sup>

<sup>1</sup>Institute of Electronic Materials Technology, Wólczyńska 133, 01-919 Warszawa, Poland

<sup>2</sup>The Andrzej Soltan Institute for Nuclear Studies, 05-400 Swierk/Otwock

*Prejem rokopisa – received: 1999-09-27; sprejem za objavo – accepted for publication: 1999-11-02*

Phase transformations and atomic transport processes characteristic for ion implanted and irradiated alloys are briefly presented and discussed. The paper starts with a short description of the basic processes occurring during ion irradiation of a solid. In the second part, some typical examples of phase transformations in ion implanted metals are presented. The next section deals with the mechanisms of atomic transport, several phenomena are discussed from simple ballistic collisions to atomic migration in non-uniform matrices containing the precipitates of insoluble atoms. Interest is focused on implanted iron-based alloys.

Key words: ion implantation, irradiation, phase transformation, atomic transport in solids

Kratka predstavitev in razprava o fazni transformaciji in procesih transporta implantiranih ionov in obsevanih zlitin. Članek začne s kratkim opisom temeljnih procesov pri jonski iradiaciji trdne snovi. V drugem delu so predstavljeni nekateri primeri različnih transformacij v ionsko implantiranih kovinah. V naslednjem delu so predstavljeni mehanizmi transporta ionov. Opisano je več pojavov, od balistične kolizije do migracije atomov v neenakomernih maticah, ki vsebujejo izločke netopnih atomov. Poudarek je na implantiranih železovih zlitinah.

Ključne besede: ionska implantacija, iradiacija, fazne transformacije, transport atomov v trdnem

### 1 INTRODUCTION

Ion implantation is a doping technique characterized by a unique feature; the impurity atoms are injected into a host matrix as highly energetic ions. Consequently, any element can be introduced into any solid target, independently of thermodynamic considerations. The method allows one to obtain a very large concentration range varying from less than  $10^{14}$  up to a few times  $10^{22}$  at./cm<sup>3</sup>. The process can be performed at any temperature. Ion implantation allows one to form at low temperature any thermodynamically stable or metastable matrix – impurity combination that may be annealed over a wide temperature range during post-implantation thermal treatments. As a consequence, this method offers a perfect tool for studying the phase transformations and atomic transport in solids.

The paper is organized as follows: first a short introduction to basic processes occurring during ion implantation is given. Next, some typical cases of phase transformations in implanted metals are presented. This part is followed by a section presenting various migration mechanisms characteristic for implanted metals. Interest is focused on iron based alloys with special attention paid to effects that are specific to ion implantation metallurgy.

### 2 DESCRIPTION OF BALLISTIC PROCESSES OCCURRING DURING ION IMPLANTATION

The incoming ion, penetrating into a solid target, loses its energy via two independent processes: inelastic collisions with target electrons and elastic collisions with target atom nuclei<sup>1-3</sup>. The first one leads to the appearance of ionized states, which in metals recombine rapidly with target electrons. In most cases when the target material is a metal (the only exceptions are irradiations in the GeV energy range) inelastic collisions lead only to target heating.

The direct collisions between ion and target nuclei (elastic collisions) may lead to high energy transfers reaching hundreds of keV i.e. largely exceeding the binding energy of atoms in solids. Such events lead to the formation of heavily damaged areas, so called collision cascades<sup>1-3</sup>. Detailed descriptions of the evolution of collision cascades can be found in numerous review papers<sup>1-4</sup>. For the purpose of the present paper it is important to note that: (i) the center of the collision cascade is enriched in vacancies whereas its periphery is characterized by a high concentration of interstitials, (ii) most of the defects annihilate within about half a picosecond of the ion impact and (iii) the energy transferred to atoms hit by ions or recoiling target atoms largely exceeds the binding energy in the crystalline structure. In most of the metals irradiated at room temperature, isolated radiation defects (vacancies or self interstitial atoms) are mobile. As a consequence, the

defects which survive the cooling phase of the collision cascade either form extended complexes or diffuse towards the closest defect sinks<sup>5</sup>.

During the early stages of cascade evolution (collisional and displacement phases<sup>1-4</sup>) more than 90% of the defects created annihilate due to the recombinations of simple Frenkel pairs. These stages can be regarded as rapid cooling of a liquid phase. Taking into account high local temperatures (~1000°C) and very short cooling times (~10<sup>-13</sup> sec) cooling rates of about 10<sup>14</sup> K/sec are expected.

The huge number of defects produced by each ion (the number of defects created by one incoming ion may reach several thousands) results in a sufficiently high concentration of the remaining defects to effectively influence the phase formation and transport mechanisms. The detailed processes strongly depend on a combination of numerous parameters (target composition, ion species, mixing enthalpy of given impurity in the host matrix<sup>6</sup>, impurity concentration, temperature, etc.) and can only be described on a case-by-case basis.

### 3 PHASE TRANSFORMATIONS IN ION IMPLANTED IRON

#### 3.1 Nitrogen implanted iron

Nitrogen implanted iron is one of the most extensively studied systems in ion implantation metallurgy<sup>7-11</sup>. The system is characterized by negative mixing enthalpy, i.e. the formation of stable phases is expected. All phases formed in the Fe-N system are crystalline. A detailed phase diagram of nitrogen implanted iron was published in Ref. 11 and is shown in **Figure 1**. One can see that the phase diagram of nitrogen implanted iron is essentially the same as the classical one<sup>12</sup>. The main difference is in the formation of almost all the phases (with the exception of the  $\gamma'$ -Fe<sub>4</sub>N phase) at room temperature. Another interesting phenomenon is the stress-induced transformation of the  $\epsilon$ -Fe<sub>3-x</sub>N to the  $\epsilon$ -Fe<sub>2</sub>N phase<sup>13</sup>. It should be pointed out that for the formation of all nitrogen-poor iron nitrides (from  $\alpha'$ -martensite to  $\epsilon$ -Fe<sub>3-x</sub>N) only relatively limited displacements of iron atoms from the original lattice positions are required. When the nitrogen concentration is too high to allow the incorporation of additional nitrogen atoms in to the structure predetermined by that of the host  $\alpha$  iron, an abrupt transformation from  $\epsilon$ -Fe<sub>3-x</sub>N nitrides into  $\epsilon$  (or  $\zeta$ )-Fe<sub>2</sub>N occurs. Indeed, each incoming nitrogen ion leads to the transformation of a large volume of Fe<sub>3-x</sub>N nitride into Fe<sub>2</sub>N<sup>14</sup>. The formation of the Fe<sub>2</sub>N phase is incomplete and even at very high nitrogen doses, about 20% of iron atoms remain in the  $\alpha$ -Fe phase<sup>14</sup>. The fact that the original metal structure persists, despite the very high nitrogen concentration, seems to be one of the peculiar characteristics of ion implantation and will be discussed in the next section.

#### 3.2 Boron implanted iron

The Fe-B system is also characterized by a negative mixing enthalpy, however, in this case the structural disorder created by incoming ions can be stabilized by boron atoms and an amorphous phase can be formed<sup>15</sup>. A detailed Mössbauer study revealed that for low and medium boron concentration the amorphous phase formed is of the composition Fe<sub>75</sub>B<sub>25</sub>, and only for very high concentration does its composition change to boron-rich phases<sup>16</sup>. Moreover, even for the highest boron doses, implanted at liquid nitrogen temperature into thin iron layers, the crystalline  $\alpha$ -Fe structure remains in the samples (**Figure 2**)<sup>16</sup>. Both effects indicate that amorphous Fe<sub>75</sub>B<sub>25</sub> phase formation is related to the segregation of boron atoms towards the vacancy-rich centers of the collisions cascades leaving a boron-free Fe envelope in the cascade periphery. The most likely explanation is that the destroyed matrix structure, in the cascade center, facilitates the formation of new phases. For the highest implantation doses, when the average B concentration exceeds 25 at.% (i.e. that of the Fe<sub>3</sub>B phase) the boron redistribution towards the center of the cascades is still maintained. As a result, one can observe the persistence of the  $\alpha$ -iron phase, similar to that observed in high-dose nitrogen-implanted iron samples.

#### 3.3 Lead implanted iron

Lead is almost completely insoluble in iron, the system is characterized by a high positive mixing enthalpy of ~250 kJ/mol<sup>5</sup>. Nevertheless, when implanted up to concentrations not exceeding 1 at.%, 90% of Pb atoms occupy substitutional positions in the iron structure (**Figure 3**)<sup>17</sup>. The mechanism leading to the incorporation of insoluble impurities in substitutional positions is rather complex and was described in detail in Ref. 5. The impurity atom is introduced into a lattice site by a replacement collision between ion and target atom. The further formation of impurity atom - vacancy complexes may displace the atom from a lattice site. Depending on the number of vacancies in the complex the impurity atom may be slightly displaced from the lattice site (complexes with one or few vacancies) or may be located in a completely random position (when complexes with many vacancies are formed). The changes in the number of vacancies in Pb-V are the origin of an increase of a substitutional fraction of Pb atoms observed for lead concentrations ranging from 0.1 to 0.4 at.% (**Figure 3**). For low implantation doses the vacancies are bonded mainly to Pb atoms, which are displaced from their lattice positions. The increase of Pb dose (hence vacancy concentration) leads to the formation of extended vacancy clusters such as dislocation loops<sup>5</sup>. The vacancies migrate from Pb-V complexes towards these defects. As a consequence, the number of vacancies in Pb-V complexes decreases,

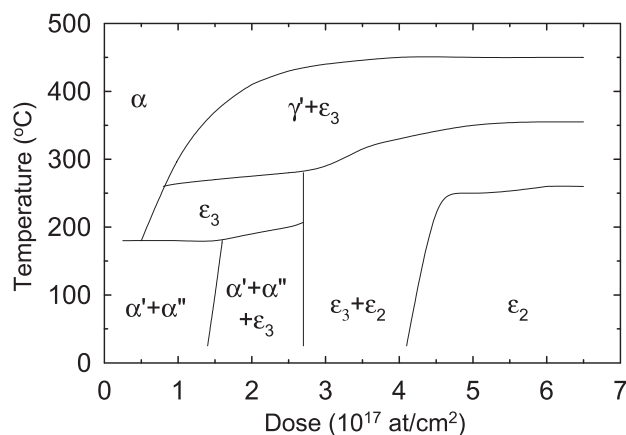


**Figure 1:** Phase diagram for nitrogen implanted iron  
**Slika 1:** Fazni diagram za železo ionsko implantirano z dušikom

leading to the return of Pb atoms to their former substitutional positions<sup>17</sup>. When the lead concentration becomes high enough, precipitation sets in and the substitutional fraction decreases rapidly. Despite the fact that no chemical reaction took place in the lead implanted iron, the FePb system with Pb atoms in substitutional positions can be regarded as an iron - lead alloy which cannot be produced in any classical process performed in thermodynamic equilibrium.

#### 4 FORMATION OF NEW PHASES BY DOUBLE IMPLANTATION INTO AN INERT MATRIX

In the previous section some examples of phase formation due to reactions between implanted impurity and host matrix atoms were described. Ion implantation also allows one to perform the reaction between two different atomic species implanted into an inert matrix. An example of such experiment was described in Ref. 18, which reports on an attempt to synthesize  $\beta$ -C<sub>3</sub>N<sub>4</sub> carbon nitride. In the study, massive doses of carbon atoms were implanted into a pure copper sample followed by nitrogen implantation. Both carbon and nitrogen atoms are insoluble in the copper, one can thus expect that in the first step carbon precipitates in the copper matrix will be formed and in the second step nitrogen atoms will be added to these precipitates. This complicated synthesis scheme has numerous advantages. First of all the synthesis occurs in heavily strained carbon precipitates, i.e. in far from equilibrium conditions. It should be noted, that when the synthesis is performed in thermodynamic equilibrium, non-covalently bonded C-N phases are preferentially formed. Secondly, the carbon precipitates were formed under a high stress which favors the formation of covalent bonds, hence a diamond-like carbon structure. Thirdly, the low nitrogen mobility in copper ensures that nitrogen atoms remain in the reaction volume and are not released from the sample. Finally, the process was performed at low temperature, which preserves the

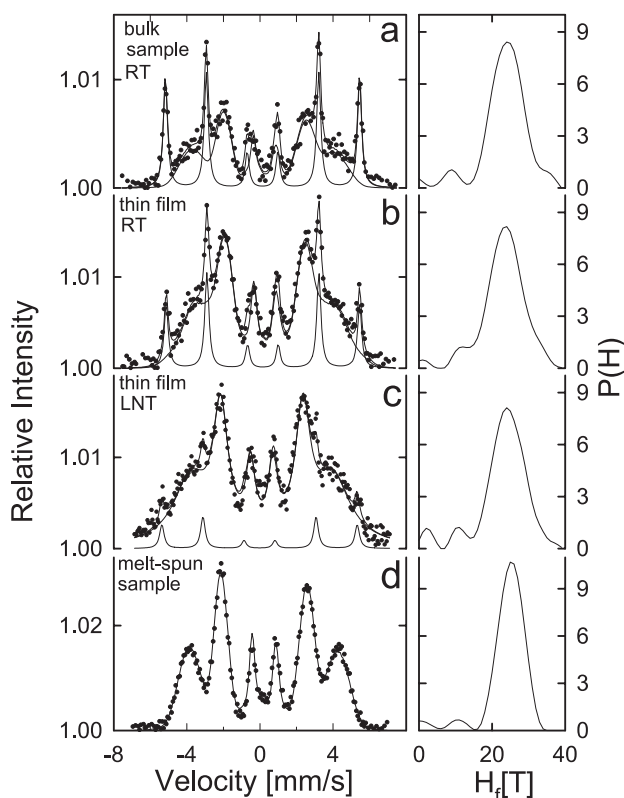


**Figure 2:** CEMS spectra and corresponding distributions of hyperfine field recorded on various B-implanted Fe samples. All samples were implanted up to the same boron concentration corresponding to the composition Fe<sub>75</sub>B<sub>25</sub>. The lines are fits to the CEMS data: one can see that the  $\alpha$ -Fe phase (narrow line Zeeman sextet) is present in all implanted samples. CEMS spectrum recorded on a melt-spun sample is included as a comparison

**Slika 2:** CEMS spektri in ustrezna porazdelitev hipermajhnih polj v različnih vzorcih železa implantiranih z B. Vsi vzorci so bili implantirani z enako koncentracijo bora, ki ustreza sestavi Fe<sub>75</sub>B<sub>25</sub>. Črte ustrezajo CEMS podatkom. Vidi se, da je  $\alpha$ -Fe faza (ozka črna Zeeman sekesteta) prisotna v vseh implantiranih vzorcih. CEMS spekter za melt-spun vzorec je dodan za primerjavo

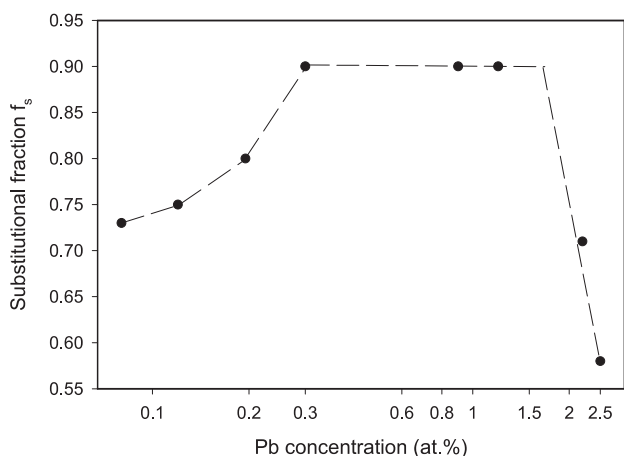


**Figure 3:** Substitutional fraction ( $f_s$ ) of Pb atoms implanted in Fe single crystals at 150 keV at RT as function of Pb concentration

**Slika 3:** Substitucijski delež ( $f_s$ ) monokristalov Fe implantiranih s Pb atomi s 150 KeV pri sobni temperaturi kot funkcija koncentracije Pb

newly formed phases against decomposition or transformation.

In the experiments described in Ref. 18 a mixture of two, covalently and non-covalently bonded C-N, phases was found. The covalently bonded nitride had a stoichiometry ranging from  $C_3N_{3.6}$  to  $C_3N_{3.9}$ , i.e. very close to that predicted by Cohen and Liu<sup>19</sup>. Once again, ion implantation showed its potential to form metastable phases which are difficult to obtain using classical techniques.

## 5 TRANSPORT MECHANISMS IN IRRADIATED ALLOYS

### 5.1 Ballistic transport

The first mechanism leading to the permanent displacement of atoms in irradiated alloys is related to the kinetic character of the implantation process itself. Incoming ions collide with target atoms transferring to them a part of their kinetic energy. The hit atoms with energy exceeding the binding energy in the solid will leave the lattice site and may be displaced sufficiently far to avoid thermal recombination with their own vacancies. This purely ballistic process is called recoil implantation and is of particular importance in ion-beam mixing studies<sup>20-22</sup>. The efficiency of ballistic transport is rather low, mainly due to a small scattering cross section for high energy collisions. Most of the displaced atoms are hit not by incoming ions but by the previously recoiled target atoms, their kinetic energy is thus low. Consequently, the range of atoms hit in secondary collisions is also small. The importance of the ballistic process relies on its kinetic nature. Recoiling atoms can be effectively injected from one layer of material to another or from the precipitate to the surrounding matrix. Isolated atoms may then diffuse within the host matrix due to thermally activated processes.

### 5.2 Thermally activated transport mechanisms

Thermally activated transport mechanisms are far more numerous. Let us start from the simplest case of an isolated impurity atom implanted into a host matrix. In such a case the general transport equation of atoms in the presence of radiation defects can be written as follows:

$$J_{\text{imp}} = -D^* \nabla N_{\text{imp}} + \alpha_{\text{imp-def}} N_{\text{imp}} J_{\text{def}} \quad (1)$$

where:  $J_{\text{imp}}$  is the impurity atom flux,  $D^*$  the impurity diffusion coefficient modified by the presence of radiation defects,  $N_{\text{imp}}$  is the concentration of impurity atoms,  $\alpha_{\text{imp-def}}$  is a constant describing the coupling between impurity atoms and radiation defects and  $J_{\text{def}}$  is the flux of defects.

A rapid survey of Eq. 1 indicates two possible driving forces of atomic migration: one defined by the impurity atoms' concentration gradient and the second determined by a flux of defects. The first mechanism is termed

Radiation Enhanced Diffusion (RED), the second one Radiation Induced Segregation (RIS)<sup>23,24</sup>. RED is a form of classical diffusion, the only difference is the increase of the diffusion coefficient. The increase is due to the presence of radiation defects that diminish the energy needed by an atom to accomplish a jump to the next position. The RIS process relies on a coupling between the impurity atoms and migrating defects (mainly vacancies). The incorporation of an additional atom into a crystalline structure creates a large stress in its vicinity. This stress can be reduced by a vacancy located close to the impurity atom. The reduction of the stress is the origin of the vacancy – impurity complexes formation in which the impurity atom follows the vacancies towards the nearest vacancy sink. One can see that the RIS mechanism may lead to the migration of an impurity against its concentration gradient that results in a local increase of impurity concentration. An example of Radiation Induced Segregation is shown in **Figure 4**, presenting the profiles of nitrogen implanted at 150°C into a thin iron layer<sup>25</sup>. The maximum of the defect concentration is located at slightly lower depths than the maximum of the impurity profile. The vacancies formed by N-implantation migrate thus mainly to the outer surface of the Fe layer dragging nitrogen atoms in this direction (squares in **Figure 4**). When the sample implanted with nitrogen at RT was postirradiated at 150°C with Ar ions having sufficiently high energy to produce the defects, mainly close to the inner interface, the defect flux was reversed and the nitrogen flux followed the change of defect migration (triangles in **Figure 4**).

A high concentration of implanted atoms may lead to the formation of various new phases. The changes in matrix phase composition can also lead to the redistribution of atoms. One of the mechanisms is related to the saturation of impurity concentration due to new phase formation. In **Figure 5** the profile of nitrogen implanted into iron up to a high concentration is shown. It is clearly seen that the nitrogen profile becomes flat in the region of highest nitrogen concentration. This effect is caused by saturation of the nitrides concentration. As a consequence, the diffusion coefficient in the region of highest nitrogen concentration increases leading to the escape of implanted atoms from this region. The implanted atoms diffuse towards the areas where the nitride formation is still possible.

Another mechanism leading to the redistribution of implanted atoms is evidenced in **Figure 6** presenting the nitrogen depth distribution profile after the N implantation into a sample preimplanted with C ions<sup>26</sup>. The energy of carbon implantation was chosen so as to create a carbon-rich layer located slightly deeper than the range of nitrogen implantation. When implanted at 150°C nitrogen atoms migrate towards the surface due to the RIS process. At 250°C the weakly bonded N-V complexes are no more stable and the RIS process

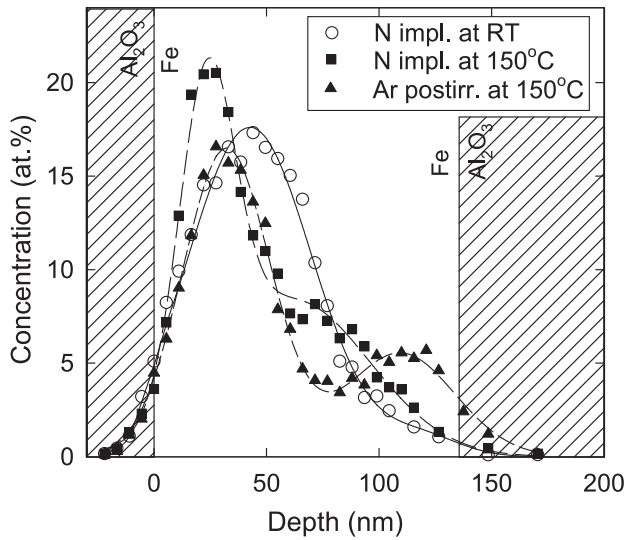


**Figure 4:** Depth distribution profiles of 50 keV nitrogen ions implanted into a thin iron layer at 150°C or implanted at RT and post-irradiated with 300 keV Ar ions at 150°C

**Slika 4:** Profil globinske porazdelitve 50 keV ionov dušika implantiranih v tanek sloj železa pri 150°C, ali implantiranih pri sobni temperaturi in nato obsevani s 300 keV ioni Ar pri 150°C

vanishes. The N atoms migrate towards the carbon-rich zone. This particular mechanism is termed Gibbs diffusion and its driving force diminishes the total free energy of the system caused by formation of strongly bonded  $\epsilon$ -Fe<sub>3-x</sub>(C,N) carbonitrides. Finally, at 300°C, the  $\epsilon$  phases are no longer stable and the  $\gamma'$ -Fe<sub>4</sub>N phase is preferentially formed. This phase cannot incorporate carbon atoms and the Gibbs diffusion driving force disappears. The N atoms are now incorporated mainly in the  $\gamma'$ -phase, formed at the maximum of the nitrogen concentration, i.e. their distribution is similar to that observed after RT implantation. The key to understanding the Gibbs diffusion is in the splitting of the population of nitrogen atoms in to two categories:

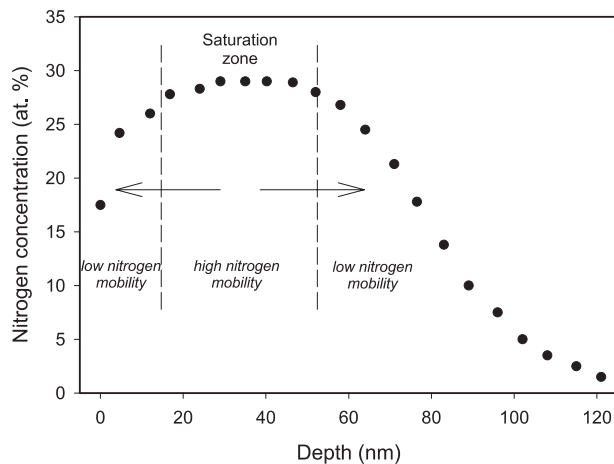


**Figure 5:** Depth distribution of 50 keV nitrogen atoms implanted into iron up to a dose of  $6 \times 10^{17}$  at./cm<sup>2</sup> at RT

**Slika 5:** Profil globinske porazdelitve 50 keV dušikovih atomov, ki so bili implantirani v železo do doze  $6 \times 10^{17}$  at./cm<sup>2</sup> pri sobni temperaturi

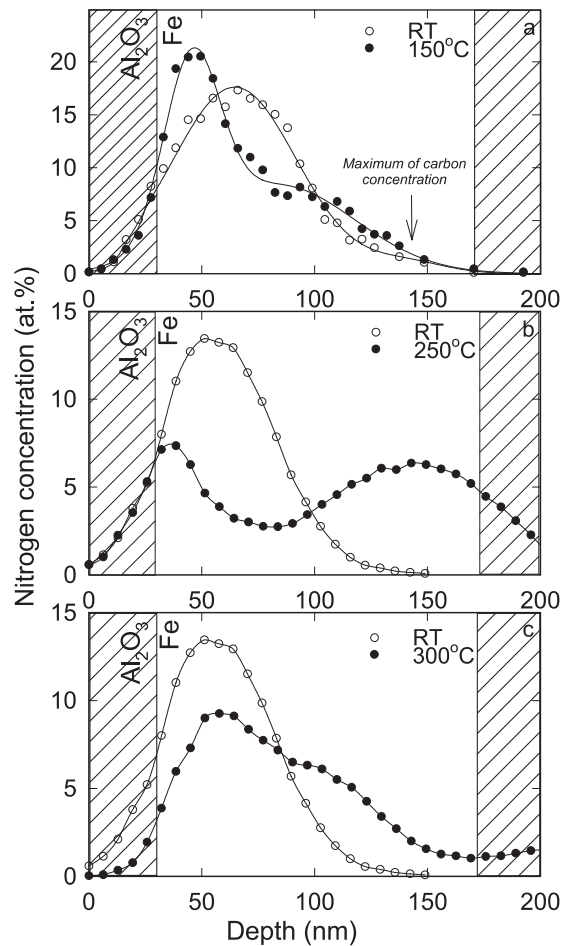


**Figure 6:** Nitrogen depth distribution profiles in iron sample pre-implanted with carbon ions

**Slika 6:** Profil globinske porazdelitve v vzorcu železa, ki je bil implantiran z ioni ogljika

unbounded N atoms freely migrating in the host Fe matrix and immobile atoms bounded in carbonitrides<sup>13</sup>. The concentration of freely migrating atoms decreases within the precipitates creating the concentration

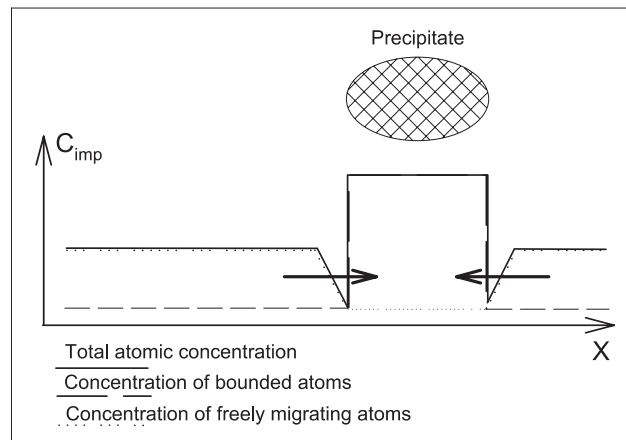


**Figure 7:** Schematic representation of Gibbs diffusion

**Slika 7:** Shematska predstavitev Gibbs-ove difuzije

gradient, driving mobile atoms towards the carbonitride precipitates, despite the fact that the total concentration of nitrogen increases in these areas. The concept of Gibbs diffusion is shown schematically in **Figure 7**.

### 5.3 Atomic transport in presence of precipitates of insoluble atoms

The great technological potential of nanostructured materials such as metallic nanoprecipitates in silica caused an enormous interest in studying this area<sup>28-31</sup>. The atomic transport in non-uniform matrices containing precipitates of insoluble atoms is a quite complex mechanism. The definitive distribution of atoms depends, in this case, on the balance between the injection of new atoms, precipitation of impurities, ejection of atoms from precipitates due to collisions with incoming ions and diffusion processes in the surrounding matrix. The process of precipitate formation has been first described by Ostwald and is called Ostwald ripening<sup>32</sup>. One can identify two major migration processes: fast small range migration of isolated atoms towards the precipitates and long range migration within the precipitate network<sup>33</sup>. The first process is rather isotropic and its influence on the depth distribution profile is very limited. The second one leads to macroscopic changes of the impurity profile width. It should be pointed out that these changes may occur in both directions, i.e. extension or shrinkage of the profile can be observed. The basic processes occurring in irradiated precipitate networks are schematically shown in **Figure 8**. The incoming ion collides with impurity atoms, confined in precipitates, leading to their ejection into a host matrix. Most of the atoms are displaced close to the precipitate boundary and return to it. Only a few are displaced sufficiently far to diffuse within the matrix to the next precipitate leading to its growth. When the precipitate reaches its saturation size the numbers of incoming and ejected atoms become equal and a new generation of precipitates is nucleated. This process leads to the macroscopic extension of the precipitate network.

The main advantage of the use of ion beams for the formation of nanostructured precipitate arrays is dependent on the delicate balance between concurrent processes. The irradiation process itself leads rather to the dissolution of the precipitates whereas thermally activated diffusion leads to precipitate growth. Consequently, by changing incoming ion mass and energy as well as the process temperature one can effectively control the size of the nanoprecipitates formed<sup>33-35</sup>. Recently, high energy ion-beam mixing has been identified as an efficient way to produce the micrometer thick SiO<sub>2</sub> layers with uniform distribution of small size Ag precipitates for optoelectronic applications<sup>36</sup>.

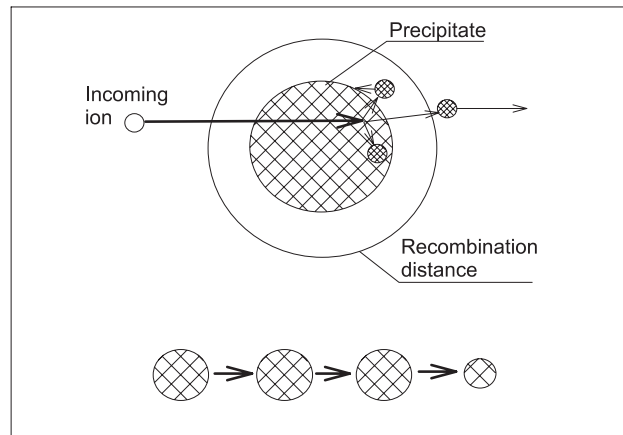


**Figure 8:** Schematic representation of processes related to the atomic transport in an irradiated alloy containing precipitates of insoluble atoms

**Slika 8:** Shematska predstavitev procesov, ki so povezani s transportom atomov v obsevani zlitini, ki vsebuje izločke netopnih atomov

## 6 CONCLUSIONS

Ion irradiation and implantation may lead to the development of various unique phenomena related to phase formation or atomic transport in solids, such as:

- formation of metastable alloys, even solid solutions of non-soluble elements;
- formation of amorphous phases;
- synthesis of new compounds over a wide concentration range;
- formation of nanostructured materials;
- defect-assisted mechanisms of atomic transport.

One of the main advantages of ion implantation is the fact that almost all process parameters (impurity concentration, temperature, atomic species, defect concentration etc.) can be independently controlled. It is thus possible to study in detail the role of one particular parameter keeping all other factors unchanged. This, together with the possibility to vary the process parameters over a very wide range, makes ion implantation a powerful tool in phase formation and atomic migration studies.

## 7 REFERENCES

- <sup>1</sup> G. Carter and J. S. Colligon, *Ion Bombardment of Solids*, Heinemann, London **1968**
- <sup>2</sup> G. Dearnaley, J. H. Freeman, R. S. Nelson and J. Stephen, *Ion Implantation*, North Holland, Amsterdam **1973**
- <sup>3</sup> The development of the current research can be followed from the Proceedings of the Conference Series *Ion Beam Modification of Materials* published in Nucl. Instr. and Meth., last proceeding published in Nucl. Instr. and Meth., B 148 (**1999**)
- <sup>4</sup> J. Jagielski, G. Gawlik, A. Zalar and M. Mozetič, *Informacije MIDE* 29 (**1999**) 2, 61
- <sup>5</sup> O. Meyer and A. Turos, *Mat. Sci. Rep.*, 2 (**1987**) 8, 1
- <sup>6</sup> A. R. Miedema, P. F. de Châtel and F. R. de Boer, *Physica B* 100 (**1980**) 1

- <sup>7</sup> Marest, *Def. and Diff. Forum*, 57-58 (1988) 273
- <sup>8</sup> N. Moncoffre, *Mater. Sci. Eng.*, 90 (1987) 99
- <sup>9</sup> A. Vredenberg, Ph. D. *Thesis*, University of Utrecht, 1991
- <sup>10</sup> M. Kopcewicz, J. Jagielski, A. Turos, and D. L. Williamson, *J. of Appl. Phys.*, 71 (1992) 9, 4217
- <sup>11</sup> B. Rauschenbach, A. Kolitsch and K. Hohmuth, *Phys. Stat. Sol.*, A 80 (1983) 471
- <sup>12</sup> H. A. Wriedt, N. A. Gocken and R. H. Hafziger, *Bulletin of Alloy Phase Diagrams* 8 (1987) 355
- <sup>13</sup> J. Jagielski, S. Fayeulle, G. Marest and N. Moncoffre, *Mat. Sci. Eng.*, A196 (1995) 213
- <sup>14</sup> J. Jagielski, G. Marest and N. Moncoffre, *Nucl. Instr. and Meth. in Phys. Res.*, B122 (1997) 575
- <sup>15</sup> A. Ali, W. A. Grant and P. J. Grundy, *Philos. Mag.* B37 (1978) 353
- <sup>16</sup> J. Jagielski, M. Kopcewicz and L. Thome, *J. Appl. Phys.*, 73 (1993) 4820
- <sup>17</sup> J. Jagielski, A. Turos and A. Dygo, *Phys. Lett. A* 133 (1988) 75
- <sup>18</sup> J. Jagielski, N. Moncoffre, P. Delichere and G. Marest, *Journ. of Mat. Science*, 34 (1999) 2949
- <sup>19</sup> A. Y. Liu and M. L. Cohen, *Science* 245 (1989) 841
- <sup>20</sup> S. Mateson and M. A. Nicolet, *Annu. Rev. Mater. Sci.*, 13 (1983) 339
- <sup>21</sup> B. M. Paine and R. S. Averbach, *Nucl. Instr. and Meth.*, B 7/8 (1985) 666
- <sup>22</sup> M. Nastasi and J. W. Mayer, *Mater. Sci. Eng.*, R12 (1994) 1
- <sup>23</sup> N. Q. Lam and H. Wiedersich, *Nucl. Instr. and Meth.*, B 18 (1987) 471
- <sup>24</sup> N. Q. Lam, P. R. Okamoto and R. A. Johnson, *J. Nucl. Mater.*, 78 (1978) 408
- <sup>25</sup> J. Jagielski, N. Moncoffre, G. Marest, L. Thome, A. J. Barcz, G. Gawlik and W. Rosinski, *J. Appl. Phys.*, 75 (1994) 153
- <sup>26</sup> J. Jagielski, N. Moncoffre, G. Marest and S. Fayeulle, *J. Appl. Phys.*, 76 (1994) 5132
- <sup>27</sup> N. Millard-Pinard, N. Moncoffre, H. Jaffrezic and G. Marest, *J. Appl. Phys.*, 74 (1993) 6032
- <sup>28</sup> P. Mazzoldi and G. W. Arnold in *Ion Beam Modification of Insulators*, Elsevier, Amsterdam 1987
- <sup>29</sup> P. D. Townsend, *Rep. Prog. Phys.*, 50 (1987) 501
- <sup>30</sup> R. H. Magruder III, J. E. Wittig, R. A. Zuhr, *J. Non-Cryst. Solids*, 163 (1993) 162
- <sup>31</sup> C. Buchal, S. Withrow, C. W. White, D. B. Poker, *Annu. Rev. Mater. Sci.*, 24 (1994) 125
- <sup>32</sup> W. Ostwald, *Z. Phys. Chem.*, 34 (1900) 495
- <sup>33</sup> S. Reiss and K-H. Heinig, *Nucl. Instr. and Meth.*, B 84 (1994) 229
- <sup>34</sup> L. Thome and F. Garrido, *Nucl. Instr. and Meth.*, B 121 (1997) 237
- <sup>35</sup> G. Bataglin, G. Della Mea, G. De Marchi, P. Mazzoldi, A. Miotello, *Nucl. Instr. and Meth.*, B 1 (1984) 511
- <sup>36</sup> L. Thome, J. Jagielski, G. Rizza, F. Garrido and J.C. Pivin, *Appl. Phys. A* 66 (1998) 327